Inorganic Chemistry – An Indian Journal

Inorganic Chemistry
ISSN: 0974-746X

Research | Vol 12 Iss 2

New Active Bisphosphonate (Etidronate) Complexes as Anticancer Agents

Fathy AA[1], Butler IS[2], Elrahman MA[3] and Mostafa SI[1*]

[1]Chemistry Department, Mansoura University, Mansoura 35516, Egypt

[2]Department of Chemistry, McGill University, Montreal QC H3A 2K6, Canada

[3]Oral Biology Department, Mansoura University, Mansoura, Egypt

[*]**Corresponding author:** Mostafa SI, Chemistry Department, Faculty of Science, Mansoura University, Egypt, Tel: 002-01008502625; Fax: 0020502246781; E-mail: sihmostafa@gmail.com

Received: November 08, 2017; **Accepted:** November 27, 2017; **Published:** December 01, 2017

Abstract

Bisphosphonates (Bps; have P-C-P moieties) are drugs that slow down or prevent bone loss. They inhibit osteoclasts, responsible for bone resorption, and allow osteoblasts, bone building cells, to be more effective; i.e., improve bone mass. Moreover, Bps are considered as anticancer drugs that cause bone damage. New complexes of etidronate disodium (Na_2Etd) with Pd (II) and Pt (II) were synthesized and characterized based on elemental analysis, molar conductivity, thermal and spectral (IR, NMR, UV-visible, mass) measurements. Their anticancer activity was tested against human prostate (DU 145) and breast (MDA-MB231) cancer cell lines compared to *Cisplatin,* the market drug.

Keywords:* *Etidronate; Palladium; Platinum; Anticancer; Spectra; Active

Introduction

Bisphosphonates, which containing P-C-P units, are used in the treatment of osteoporosis, Paget's disease of bone and to decrease the high calcium levels in cancer patients [1,2]. They are divided into two categories are: nitrogenous bisphosphonates (palmidronate, alendronate and zoledronate) and non-nitrogenous bisphosphonates (etidronate, clodronate and tiludronate) [3]. They show different mechanism of action in the treatment of osteoclast cells. Many cancers that affect bones are usually started in another organ in the body, followed by spreading to the bone; i.e., secondary bone cancer. These are breast, prostate and lung cancer, and myeloma. Some types of cancer treatment can also affect the bones making them

weaker, including chemotherapy and hormone therapies. Bisphosphonates are types of drugs that can help in the treatment some types of cancer that cause bone damage [2].

Etidronate disodium (Na_2Etd; FIG. 1) is used to prevent osteoporosis which caused by corticosteroids (medicine may cause osteoporosis). Etidronate is also used for treating Paget's disease of bone as well as heterotopic ossification (growth of bone tissue in an area of the body other than the skeleton) in people who have had total hip replacement surgery or an injury to the spinal cord. It works on the base of slowing the breakdown of old bone with the formation of new one [4].

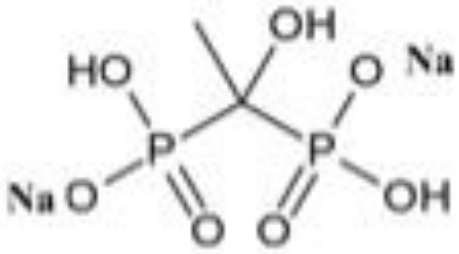

FIG. 1. **Etidronate disodium (Na_2Etd).**

Spectrophotometric determination of Etd^{-2} in pharmaceuticals, based on its oxidation with potassium persulfate and reaction of the generated orthophosphate ions with molybdovanadate reagent have been reported [5]. It is known that upon complexation, the pharmacological properties are improved due to the action by combination of chelate and metal ion biological properties [6-8]. The preparation and X-ray structure of some Zn (II), Cd (II), Ca (II), Ba (II), Sr (II) and Mg (II) complexes of Bps have been have been reported [9-21]. This article is dealing with the preparation of Pd (II) and Pt (II) etidronate complexes. Their structure was characterized using IR, NMR, UV-visible, mass spectra, elemental analysis, molar conductivity and thermal measurements. The complexes were tested against human prostate (DU 145) and breast (MDA-MB231) cancer cell lines compared with *Cisplatin*.

Experimental

Materials

All reagents and solvents were purchased from Alfa/Aesar and all manipulations were performed under aerobic conditions using materials and solvents as received. All the reagents and solvents purchased commercially were used without further purification. DMSO-d_6 was used for the NMR measurements referenced against TMS.

The human prostate cancer (DU 145) and breast cancer (MDA-MB231) cell lines were obtained from the American Type Culture Collection (ATCC catalog number). Cells were maintained in RPMI media from Wisent Bio Products, which was

supplemented with Fetal Bovine Serum (FBS; 10%), HEPES (12 mL), L-glutamine (5 mL), gentamicin sulfate (500 µL), fungisone (250 µL) and ciprofloxacin (170 µL). The bio-products were purchased from Wisent Inc. The cells were grown in corning cell cultured treated polystyrene flasks, placed in an incubator at 37°C and CO_2 level of 5%. The media of each flask were changed when necessary and cell passaging was done between 85% and 95% confluence.

Measurements

Elemental analyses (C, H, N) were performed in Microanalytical Unit, Cairo University. Infrared spectra were recorded on a Nicolet 6700 Diamond ATR spectrometer in the 4000 cm^{-1}-200 cm^{-1} range. NMR spectra were measured on Varian Mercury 200 MHz, 300 MHz and 500 MHz spectrometer. NMR spectra were recorded on VNMRS 200 and 500 MHz spectrometer in DMSO d_6 using TMS as reference. Mass spectra (ESI-MS) were recorded using LCQ Duo and double focusing MS25RFA instruments, respectively. Electronic spectra were recorded in DMF using a Hewlett-Packard 8453 spectrophotometer. Thermal analysis measurements were made in the 20°C-1000°C range at a heating rate of 20°C min^{-1} using Ni and NiCo as references, on a on a TA instrument TGA model Q500Analyzer TGA-50. Molar conductivity measurements were carried out at room temperature on a YSI Model 32 conductivity bridge.

Preparations

[Pt $(NaEtd)_2$].$2H_2O$: Aqueous solution of K_2PtCl_4 (0.1037 g, 0.25 mmol; 7.5 mL) was added to etidronate disodium (0.125 g, 0.5 mmol). The reaction mixture was heated under reflux with stirred for 18 h. The deep brown solution was reduced in volume and brown precipitate was obtained. It was filtered off, washed with water and air dried. Conductivity data (10^{-3} M in DMF): Λ_M=16.0 ohm^{-1} cm^2 mol^{-1}. Anal. Calcd. For $C_4H_{16}Na_2O_{16}P_4Pt$: C, 7.0; H, 2.3, P, 18.1%; Found: C, 6.9, H, 2.4, P, 18. 3%. IR (KBr, cm^{-1}); ν(P=O), 1212; ν(P-O), 1122; ν(Pt-O), 555. ^{1}H NMR (400 MHz, DMSO-d_6): H (ppm); 2.49 (3H, -CH_3), 5.33 (H, -OH). ^{31}P NMR (200 MHz, DMSO-d_6): p (ppm); 19.33. ESI-MS (*m/z*): 648.88 for [Pt $(NaEtd)_2$]$^+$.

[Pd (Etd) $(H_2O)_2$]: The same procedure of the Pt (II) analogue was applied, using K_2PdCl_4 (0.08 g, 0.25 mmol). Conductivity data (10^{-3} M in DMF): Λ_M=20.4 ohm^{-1} cm^2 mol^{-1}. Anal. Calcd. For $C_2H_{10}O_9P_2Pd$: C, 6.9; H, 2.9, P, 17.9; Pd, 30.7%; Found: C, 7.1, H, 3.00, P, 17. 6; Pd, 30.9%. IR (KBr, cm^{-1}); ν(P=O), 1225; ν(P-O), 1122; ν(P-O), 1170; ν(Pd-O), 534. ^{1}H NMR (400 MHz, DMSO-d_6): H (ppm); 2.48 (3H, -CH_3), 5.46 (H, -OH). ^{31}P NMR (200 MHz, DMSO-d_6): p (ppm); 18.87. ESI-MS (*m/z*): 311.5 for [Pd (Etd)]$^+$.

Anticancer activity

Cell culture: Human prostate (DU 145) and breast (MDA-MB231) cancer cell lines were maintained in RPMI media from Wisent Bio Products, which was supplemented with Fetal Bovine FBS; 10% Serum, 12 mL HEPES, 5 mL L-glutamine, 500

µL gentamicin sulfate, 250 µL fungisone and 170 µL ciprofloxacin. The cells were grown in corning cell cultured treated polystyrene flasks, which placed in an incubator at 37°C and CO_2 level of 5%. The media of each flask was changed when necessary and cell passaging was done between 85% and 95% confluence.

Complexes treatment: In all assays, complexes stocks, [Pd (Etd) $(H_2O)_2$] and [Pt $(NaEtd)_2$] 0.3125×10^{-2} to 100 µM were prepared by dissolving in DMSO to ensure complete dissolution.

***In vitro* growth inhibition essays:** The growth inhibiting effects on human prostate cancer (DU 145) and breast cancer (MDA-MB231) cell lines were examined *in vitro* and the results were compared against negative and positive controls. Both human prostate cancer (DU 145) and breast cancer (MDA-MB231) cell lines were grown to 80% confluence and then incubated in RPMI media onto 96-well plates (corning Inc.) with 3000-5000 cells per well (100 µL medium/well) density. They were allowed to attach for 24 h. treated with a wide range of the complexes concentration range (0.3125×10^{-2}-100 µM). The treatment was done in triplicate for 5 days in the incubator. The cells were fixed with cold trichloroacetic acid (50 µL, 50%) for 2 h at 4°C. Using flow of water, the wells were rinsed four times, dried well as much as possible and stained with Sulforhodamine B (SRB; 50 µL, 0.4 g/100 mL) for at least 1 h. at RT. Subsequently, the SRB was rinsed with 1% acetic acid and air-dried overnight. Finally, the dye was dissolved in Tris-base (10 mM, pH=10-10.5; 200 µL) for 2-5 min on a shaking platform. The optical density for each well was recorded using a microplate reader (model 2550; Bio-Rad) at 492 nm [22]. Each complex concentration was run in triplicate in at least two independent experiments. The readings were analyzed using the GraphPad Prism program (GraphPad software, Inc.), and a sigmoidal dose-response curve was used to determine the 50% inhibitory concentration (IC_{50}) [22].

Results and Discussion

The elemental analyses (C, H, P, Pd) for the complexes are in agreement with the assigned formulae and the molar conductivities (Λ_M) in DMF at room temperature suggest the non-electrolytic nature of the complexes [23,24]. The new complexes are stable under normal laboratory conditions and soluble in DMF and DMSO.

IR spectra

The IR spectrum of Na_2Etd shows multiple absorptions at 3600-3300 cm^{-1} can be attributed to ν(OH) stretching of P–OH and C–OH units. The bands appear at 1234 cm^{-1} and 1183 cm^{-1} attributable to ν(P=O) and ν(P-O) stretches, respectively [25,26]. Upon complexation, the ν(P-O) stretch was shifted to lower wave number (1122 cm^{-1}). The ν_{as}(P-O) and ν_s(P-O) stretching vibrations are observed at 1055 cm^{-1} and (1019, 915) cm^{-1}, respectively. The vibrations of P=O and P-O(H) groups show bands in the region below 1320 cm^{-1}. In case of Pt (II) complex, both ν(P=O) and ν(P-O) stretches were shifted

to lower wave number; i.e., coordination occurs through P=O and deprotonated P-O^- oxygen atoms [27,28]. Extra band is observed near 540 cm^{-1} assigned to ν(M-O) stretch [23,24,29]. FIG. 2 and 3 show the structure of [Pt $(NaEtd)_2$] and [Pd (Etd) $(H_2O)_2$], and the IR spectrum of [Pd (Etd) $(H_2O)_2$], respectively.

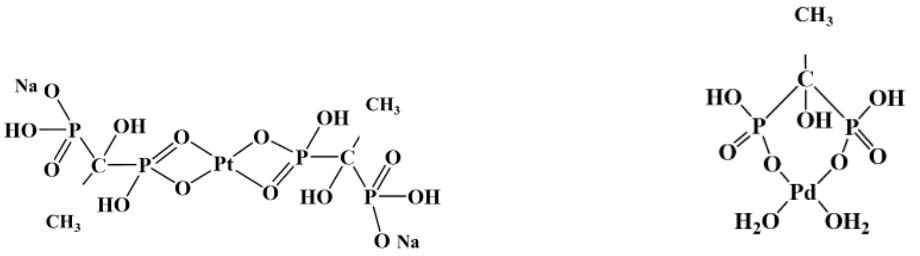

FIG. 2. **Structure of [Pt $(NaEtd)_2$] and [Pd (Etd) $(H_2O)_2$].**

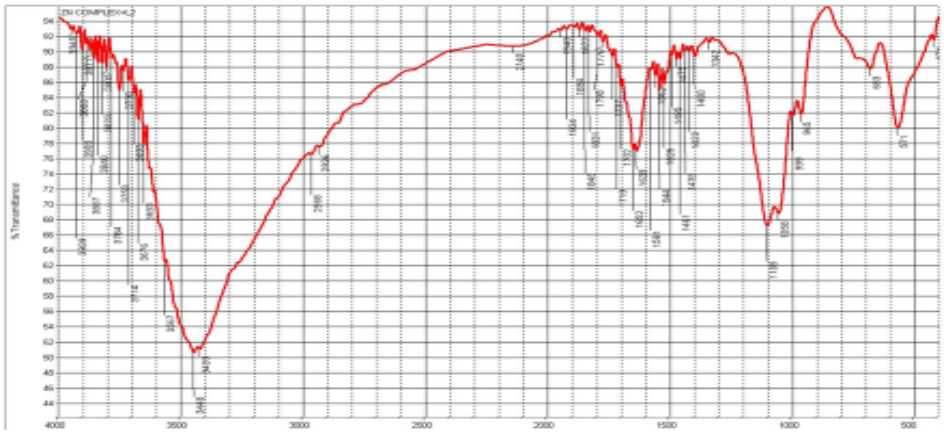

FIG. 3**. IR spectrum of [Pd (Etd) $(H_2O)_2$].**

NMR spectra

The ^1H NMR spectrum of Na_2Etd exhibits a broad singlet at δ 5.31 ppm attributed to OH (C-OH), while that at δ 2.23 ppm, is assigned to CH_3 [30,31]. The later band is shifted to ~ δ 2.50 ppm upon complex formation (FIG. 4a).

The ^{31}P NMR spectrum of Na_2Etd exhibits single resonance at 15.69 ppm. In the complexes, this resonance is shifted to lower filed (near δ 19.0 ppm; FIG. 4b), indicating the participation of P-O oxygen atoms in coordination.

UV-visible spectra

The UV-visible spectrum of the diamagnetic complexes exhibits bands near 470 nm and 325 nm (FIG. 5) due to $^1A_{1g} \rightarrow {}^1B_g$ and $^1A_{1g} \rightarrow {}^1E_g$ transitions, respectively, showing in a square-planar configuration [24,29].

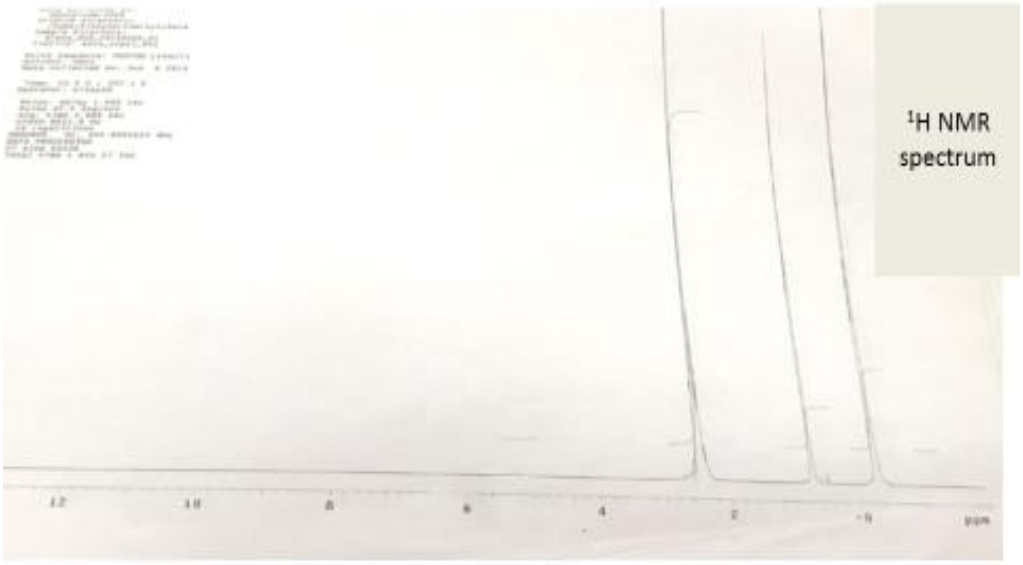

FIG. 4a. **Spectrum of [Pd (Etd) $(H_2O)_2$].**

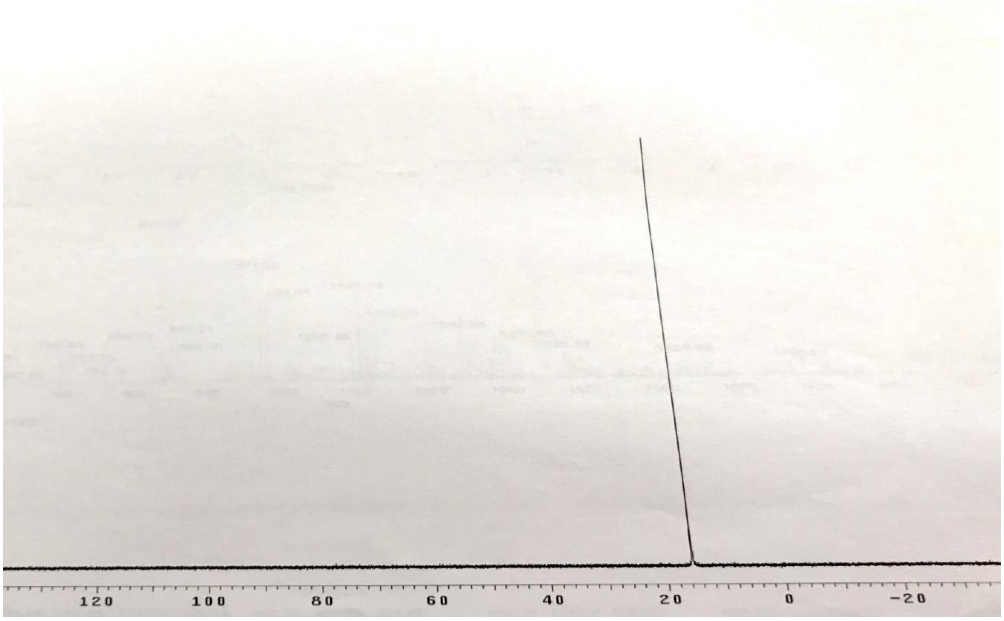

FIG. 4b. **^{31}P NMR spectrum of [Pd (Etd) $(H_2O)_2$].**

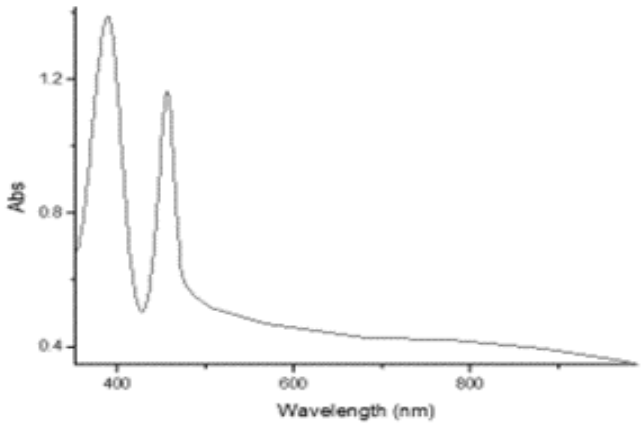

FIG. 5. **The UV-visible spectrum of [Pd (NaEtd)$_2$].**

Mass spectra

To Confirm the formulation of the complexes, [Pt (NaEtd)$_2$] and [Pd (Etd) (H_2O)$_2$], their mass spectra show the including the molecular ions [Pt (NaEtd)$_2$]$^+$ and [Pd (Etd)]$^+$ (FIG. 6**)** at *m/z* 648.88 and 311.5, respectively [23,24].

TGA studies

The thermal decomposition of both [Pt (NaEtd)$_2$].2H_2O and [Pd (Etd) (H_2O)$_2$] complexes paths (below 130°C) with evaluation of the crystal water content [23,24]. The thermograms of [Pt (NaEtd)$_2$].2H_2O shows the first step weight loss corresponds to the loss of hydrated waters molecules (5.3%). The second step (111°C-453°C), due to the release of two $C_2H_5O_4PNa$ species (42.8%), leaving a residue with 51.6%. The thermogram of [Pd (Etd)H_2O)$_2$] shows TG inflection in the ranges 121-299 and 300°C-780°C, assigned to the elimination of coordinated water (10.3%) and (C_2H_4O, 2O_2) (31.34) fragments, respectively, leaving residue of 58.9% [23,24,29].

Anticancer activity

Cancers that spread to the bones damage the bones and release proteins that interfere with the normal bone shaping process. The proteins stimulate the cells that break down bone (osteoclasts) and make them overactive. Since bone is destroyed faster than rebuilt and calcium is normally stored in the bones, the breakdown of bone cells releases more calcium than usual into the blood [4].

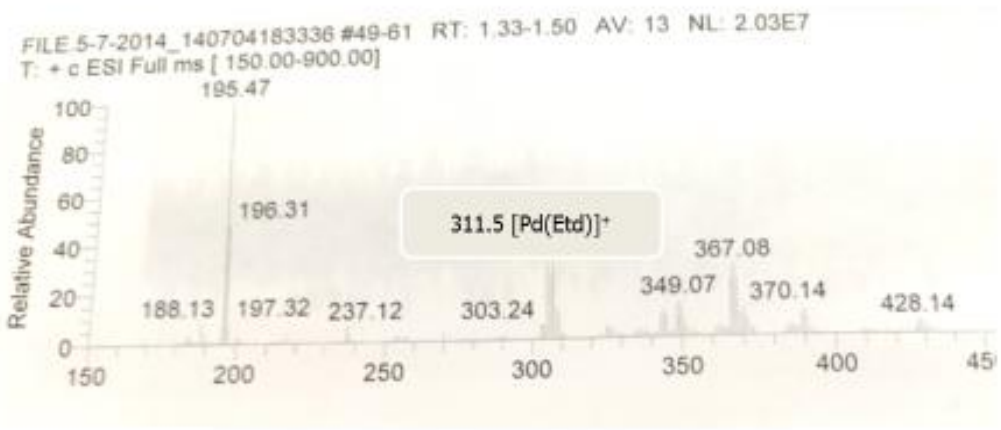

FIG. 6. **Mass Spectra of [Pd (Etd) (H_2O) Cl].**

Many studies have clearly demonstrated that *in vitro* bisphosphonates exert cytostatic and pro-apoptotic effects on breast and prostate cancer cell lines similar to those with myeloma cell lines. The viability of breast cancer cell lines cultured *in vitro* with zoledronic acid, as anticancer agent, was more potent than pamidronate, and clodronate. Increasing apoptosis was convincingly based on changing of nuclear morphology, DNA fragmentation, down-regulation of bcl-2, and proteolysis of poly-APD-ribose polymerase [27-32].

In vitro anticancer activity of both [Pt ($NaEtd)_2$] and [Pd (Etd) ($H_2O)_2$] against human prostate (DU 145) and breast (MDA-MB231) cancer cell lines was examined, with *Cisplatin*; as positive control. The antitumor activities were quantified by the corresponding IC_{50} values (FIG. 7; TABLE 1). The complex [Pt ($NaEtd)_2$] shows high inhibition against DU 145 and MDA-MB231 human cancer cell lines. The IC_{50} values were 2.00 ± 0.2 and 1.76 ± 0.3 µM, respectively. The IC_{50} values of *Cisplatin* were 2.21 ± 0.5 and 3.20 ± 0.5 µM, respectively.

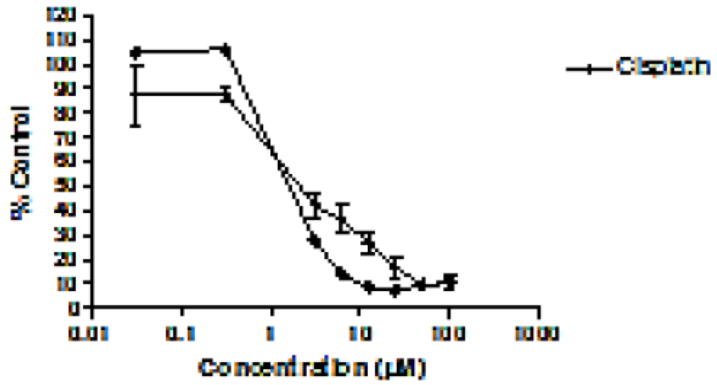

FIG. 7. **IC_{50} of [Pt ($NaEtd)_2$] against breast MDA-MB231 human cancer cell line.**

Since the DNA is the main target of the drug, the anticancer activity is related to the DNA-binding ability. The difference between the anticancer activity of [Pt $(NaEtd)_2$] and *Cisplatin* is based on the binding ability of DNA and cancer cell uptake [24,29]. Moreover, the cell viability of both [Pt $(NaEtd)_2$] and [Pd (Etd) $(H_2O)_2$] against human prostate and breast cancer cell lines showed high selectivity of [Pt $(NaEtd)_2$] rather than human prostate and breast normal cell lines (TABLE 1).

TABLE 1. **Anticancer activity of Na_2Etd and its complexes against the human prostate (DU 145) and breast cancer (MDA-MB231) cell lines[*].**

Compounds	**IC_{50} μM breast cancer (MDA-MB231) cell line**	**Selectivity breast normal (MDA-MB231) cell line**	**IC_{50} μM human prostate cancer (DU 145) cell line**	**Selectivity breast normal (DU 145) cell line**
Na_2Etd	45.31 ± 0.3	-	46.99 ± 0.3	-
[Pt $(NaEtd)_2$]	1.76 ± 0.3	91.76	2.00 ± 0.2	89.38
[Pd (Etd) $(H_2O)_2$]	4.85 ± 0.4	67.21	5.32 ± 0.3	54.56
Cisplatin	3.20 ± 0.5		2.21 ± 0.5	

[*]Selectivity of drugs towards normal cell lines are underlines

Conclusion

Two Pt (II) and Pd (II) etidronate complexes were prepared and characterized using IR, NMR, UV-visible, mass, elemental analysis, molar conductivity and thermal analysis. The complex, [Pt $(NaEtd)_2$] shows high anticancer activity against the human prostate (DU 145) and breast (MDA-MB231) cancer cell lines, and higher than the market drug *Cisplatin*.

Acknowledgments

This research is funded by the High Ministry of Education, Post 2014 and BRIDGES-Development-3 Project; Scientific Research Academy, Ministry of Research, Egypt.

REFERENCES

1. Vasikaran SD. Bisphosphonates: An overview with special reference to alendronate. Ann Clin Biochem.
2. Fleisch H, Bisaz S. Isolation from urine of pyrophosphate, a calcification inhibitor. Am J Physiol. 1962;203(4):671-5.

3. Rogers MJ, Gordon S, Benford HL, et al. Cellular and molecular mechanisms of action of bisphosphonates. Cancer. 2000;88(S12):2961-78.
4. De Rosa G, Misso G, Salzano G, et al. Bisphosphonates and cancer: What opportunities from nanotechnology? Journal of Drug Delivery. 2013, ID 637976,17.
5. Walash MI, Metwally ME, Eid MI, et al. Spectrophotometric Determination of Risedronate and Etidronate in Pharmaceutical Formulations *via* the Molybdovanadate Method. Analytical Letters. 2009;42(11):1571-87.
6. Hambley TW. Developing new metal-based therapeutics: Challenges and opportunities. Dalton Trans. 2007(43):4929-37.
7. Navarro M, Gabbiani C, Messori L, et al. Metal-based drugs for malaria, trypanosomiasis and leishmaniasis: Recent achievements and perspectives. Drug Discovery Today. 2010;15(23):1070-8.
8. Fricker SP, Mosi RM, Cameron BR, et al. Metal compounds for the treatment of parasitic diseases. J Inorg Biochem. 2008;102(10):1839-45.
9. Serre C, Férey G. Hydrothermal synthesis, structure determination from powder data of a three-dimensional zirconium diphosphonate with an exceptionally high thermal stability: Zr (O 3 P-(CH 2)-PO 3) or MIL-57. J Mater Chem. 2002;12(8):2367-9.
10. Finn RC, Lam R, Greedan JE, et al. Solid-State Coordination Chemistry: Structural Influences of Copper− Phenanthroline Subunits on Oxovanadium Organophosphonate Phases. Hydrothermal Synthesis and Structural Characterization of the Two-Dimensional Materials [Cu (phen) (VO) ($O_3PCH_2PO_3$) (H2O)], [{Cu (phen)} 2 (V_2O_5) ($O_3PCH_2CH_2PO_3$)], and [{Cu (phen)} 2 (V_3O_5) ($O_3PCH_2CH_2CH_2PO_3$) 2 (H_2O)] and of the Three-Dimensional Phase [{Cu (phen)} 2 (V_3O_5) ($O_3PCH_2PO_3$) 2 (H_2O)]. Inorg. Chem. 2001;40(15):3745-54.
11. Yin P, Peng Y, Zheng LM, et al. Syntheses and structures of layered copper (II) diphosphonates with mixed ligands. Eur J Inorg Chem. 2003;(4):726-30.
12. Barthelet K, Merlier C, Serre C, et al. Microporous hybrid compounds: Hydrothermal synthesis and characterization of two zinciomethylenediphosphonates with 3D structures, structure determination of their dehydrated forms. J Mater Chem. 2002;12(4):1132-7.
13. Barthelet K, Riou D, Férey G. Hydrothermal synthesis and structure determination of Na_2Zn {O 3 P□ CH 2□ PO 3}. H 2 O (MIL-58): A new zincomethylenediphosphonate exhibiting a hybrid zeotype. Solid State Sci. 2002;4(6):841-4.
14. Sergienko VS, Aleksandrov GG, Afonin EG. Crystal structure of triethanolammonium bis (1-hydroxyethane-1, 1-diphosphonato) diaquazincate pentahydrate, [($OHCH_2CH_2$) 3NH] [Zn (H_2O) 2 ($H_{2\cdot5}$ L) 2] · $5H_2O$. Afonin, Kristallografiya. 2000;45(2):230-3.
15. Berenson JR. Treatment of hypercalcemia of malignancy with bisphosphonates. Semin Oncol. 2002;29(6):12-8.
16. Coleman RE. Bisphosphonates: Clinical experience. The Oncologist. 2004;9:14-27.
17. Kontturi M, Peräniemi S, Vepsäläinen JJ, et al. A structural study of bisphosphonate metal complexes: Three new polymeric structures of the calcium complex of clodronic acid. Inorg Chem. 2004(13):2627-31.
18. Kontturi M, PeraÈniemi S, Vepsaelaeinen JJ, et al. Poly [[tetraaqua (μ7-hydrogen dichloromethylenebisphosphonato) (μ5-hydrogen dichloromethylenebisphosphonato) tribarium (II)] monohydrate]. Acta Crystallogr. 2004;60(11):592-4.
19. Kontturi M, PeraÈniemi S, Vepsaelaeinen JJ, et al. Pentaaqua (dichloromethylenebisphosphonato) strontium (II). Acta Cryst. 2004:1060-62.

20. Kontturi M, Laurila E, Mattsson R, et al. Structures of bisphosphonate metal complexes: Zinc and cadmium complexes of clodronate and its partial ester derivatives. Inorg Chem. 2005;44(7):2400-6.
21. Simchi A, Tamjid E, Pishbin F, et al. Recent progress in inorganic and composite coatings with bactericidal capability for orthopaedic applications. Nanomed Nanotechnol Biol Med. 2011;7(1):22-39.
22. Skehan P, Storeng R, Scudiero D, et al. New colorimetric cytotoxicity assay for anticancer-drug screening. JNCI: J Natl Cancer Inst. 1990;82(13):1107-12.
23. El-Asmy HA, Butler IS, Mouhri ZS, et al. Zinc (II), ruthenium (II), rhodium (III), palladium (II), silver (I), platinum (II) and complexes of 2-(2′-hydroxy-5′-methylphenyl)-benzotriazole as simple or primary ligand and 2, 2′-bipyridyl, 9, 10-phenanthroline or triphenylphosphine as secondary ligands: Structure and anticancer activity. J Mol Struct. 2014;1059:193-201.
24. Shabana AA, Butler IS, Gilson DF, et al. Synthesis, characterization, anticancer activity and DNA interaction studies of new 2-aminobenzothiazole complexes; crystal structure and DFT calculations of [Ag $(Habt)_2$] ClO 4. Inorg Chim Acta. 2014;423:242-55.
25. Du XL, Zhang TL, Yuan L, et al. Complexation of ytterbium to human transferrin and its uptake by K562 cells. The FEBS Journal. 2002;269(24):6082-90.
26. Juribašić M, Tušek-Božić L. Spectroscopic and DFT study of 3-quinolyl-α-aminophosphonates. J Mol Struct. 2009;924:66-72.
27. Demoro B, Caruso F, Rossi M, et al. Risedronate metal complexes potentially active against Chagas disease. J Inorg Biochem. 2010;104(12):1252-8.
28. Demoro B, Caruso F, Rossi M, et al. Bisphosphonate metal complexes as selective inhibitors of Trypanosoma cruzi farnesyl diphosphate synthase. Dalton Transactions. 2012;41(21):6468-76.
29. El-Asmy HA, Butler IS, Mouhri ZS, et al. Synthesis, characterization and DNA interaction studies of new complexes containing 2-mercaptobenzothiazole and different dinitrogen or phosphorous aromatic donors. Inorganica Chim Acta. 2016;441:20-33.
30. Deacon GB, Greenhill NB, Junk PC, et al. Synthesis and crystal structure of lithium alendronate. Journal of Coordination Chemistry. 2011;64(1):179-85.
31. L Qiu, H Liu, K Li, et al. Preparation and Biological Evaluation of Two Novel Platinum (II) Complexes Based on the Ligands of Dipicolyamine Bisphosphonate Esters. Molecules. 2016: 255-267.
32. Senaratne SG, Pirianov G, Mansi JL, et al. Bisphosphonates induce apoptosis in human breast cancer cell lines. British Journal of Cancer. 2000;82(8):1459-68.